ISSN 1674-1056
http://cpb.iphy.ac.cn
http://iopscience.iop.org/cpb
中国物理 B
Chinese Physics
中国物理
Chinese Physics B

Weak wide-band signal detection method based on small-scale periodic state of Duffing oscillator

Jian Hou(侯健), Xiao-pengYan(闫晓鹏), Ping Li(栗苹), Xin-hong Hao(郝新红)
Citation: Chin. Phys. B . 2018, 27(3): 030702. **doi:** 10.1088/1674-1056/27/3/030702

Journal homepage: http://cpb.iphy.ac.cn; http://iopscience.iop.org/cpb

What follows is a list of articles you may be interested in

Generalized Chaplygin equations for nonholonomic systems on time scales

Shi-Xin Jin(金世欣), Yi Zhang(张毅)
Chin. Phys. B . 2018, 27(2): 020502. **doi:** 10.1088/1674-1056/27/2/020502

Topological horseshoe analysis and field-programmable gate array implementation of a fractional-order four-wing chaotic attractor

En-Zeng Dong(董恩增), Zhen Wang(王震), Xiao Yu(于晓), Zeng-Qiang Chen(陈增强), Zeng-Hui Wang(王增会)
Chin. Phys. B . 2018, 27(1): 010503. **doi:** 10.1088/1674-1056/27/1/010503

A circular zone counting method of identifying a Duffing oscillator state transition and determining the critical value in weak signal detection

Li Meng-Ping, Xu Xue-Mei, Yang Bing-Chu, Ding Jia-Feng
Chin. Phys. B . 2015, 24(6): 060504. **doi:** 10.1088/1674-1056/24/6/060504

Fast filtering algorithm based on vibration systems and neural information exchange and its application to micro motion robot

Gao Wa, Zha Fu-Sheng, Song Bao-Yu, Li Man-Tian
Chin. Phys. B . 2014, 23(1): 010701. **doi:** 10.1088/1674-1056/23/1/010701

Application of local polynomial estimation in suppressing strong chaotic noise

Su Li-Yun,Ma Yan-Ju,Li Jiao-Jun
Chin. Phys. B . 2012, 21(2): 020508. **doi:** 10.1088/1674-1056/21/2/020508

Weak wide-band signal detection method based on small-scale periodic state of Duffing oscillator*

Jian Hou(侯健), Xiao-peng Yan(闫晓鹏)†, Ping Li(栗苹), and Xin-hong Hao(郝新红)

Science and Technology on Electromechanical Dynamic Control Laboratory, School of Mechatronical Engineering, Beijing Institute of Technology, Beijing 100081, *China*

(Received 16 August 2017; revised manuscript received 4 December 2017; published online 13 February 2018)

The conventional Duffing oscillator weak signal detection method, which is based on a strong reference signal, has inherent deficiencies. To address these issues, the characteristics of the Duffing oscillator's phase trajectory in a small-scale periodic state are analyzed by introducing the theory of stopping oscillation system. Based on this approach, a novel Duffing oscillator weak wide-band signal detection method is proposed. In this novel method, the reference signal is discarded, and the to-be-detected signal is directly used as a driving force. By calculating the cosine function of a phase space angle, a single Duffing oscillator can be used for weak wide-band signal detection instead of an array of uncoupled Duffing oscillators. Simulation results indicate that, compared with the conventional Duffing oscillator detection method, this approach performs better in frequency detection intervals, and reduces the signal-to-noise ratio detection threshold, while improving the real-time performance of the system.

Keywords: Duffing oscillator, weak signal detection, stopping oscillation system, small-scale periodic state

PACS: 07.50.Qx, 05.45.–a, 43.60.Hj, 05.45.Jn **DOI:** 10.1088/1674-1056/27/3/030702

1. Introduction

Research on weak signal detection is very important in many fields.[1,2] Traditional weak signal detection methods primarily involve the filtering of noise, but these methods can potentially alter the useful signal during this process. Therefore, in general, when the signal-to-noise ratio (SNR) is less than −10 dB, it is difficult to extract weak signals against a background of noise.[3] Chaotic systems are different from the traditional methods in that they are immune to noise and sensitive to a specific signal, which means that they are particularly suitable for weak signal detection under noisy conditions.[4–7]

The Duffing oscillator is one of the classic nonlinear systems that have been extensively studied for weak signal detection.[8–11] In addition, many researchers have investigated the combination of Duffing oscillators and other detection methods for weak signal detection with positive results.[12–14] The effectiveness of these approaches under a low SNR has been investigated both experimentally and theoretically.[15] Based on the intermittency transition between order and chaos, the detection and estimation of a weak signal with unknown frequency can be quantitatively studied.[16] As this method has been validated earlier, numerous additional studies have been performed with regard to the efficiency of the approach. For instance, using two coupled Duffing oscillator systems, harmonious wave and square wave signals can be detected under a strong colored noise background.[17] Combining chaos theory with cross-correlation detection, a weak signal can be detected when the SNR is reduced to −77 dB.[18] All of the Duffing oscillator detection methods in Refs. [16]–[18] addressed the low-frequency weak signals, and did not consider large-bandwidth high-frequency signals. However, the SNR detection threshold of Duffing oscillator systems deteriorates rapidly with the irregularity and increase of the weak signal frequency. Therefore, a Duffing oscillator capable of detecting weak signals with arbitrary frequencies needs to be investigated.

An extended Duffing oscillator model was used to effectively detect weak high-frequency partial discharge signals.[19] A weak signal detection approach based on the generalized parameter-adjusted SR (GPASR) model is proposed.[20] By combining the advantages of FPGA and the Duffing oscillator, a novel state detector, phase trajectory auto-correlation, is introduced for state detection of Duffing oscillators.[21] The Duffing oscillator systems in Refs. [19]–[21] eliminated the limitation of small frequency parameters. It should be noted that all the Duffing oscillator detection methods previously mentioned are based on a strong reference signal, i.e., they depend on the phase transition from chaotic to large-scale periodic motion. However, this phase transition process is difficult to identify accurately, and the critical threshold corresponding to the critical state is greatly affected by many factors.[22] In addition, the inherent deficiencies of the conventional Duffing oscillator detection method, which is based on a strong refer-

*Project supported by the National Natural Science Foundation of China (Grant No. 61673066).

†Corresponding author. E-mail: yanxiaopeng@bit.edu.cn

© 2018 Chinese Physical Society and IOP Publishing Ltd

ence signal, were not considered.[23]

In this investigation, our objective was to maximize the frequency detection interval of a single Duffing oscillator, while avoiding the effects of the inherent deficiencies of this method on the detection accuracy. Firstly, based on the theory of the stopping oscillation system, which is sensitive to a certain driving force and immune to a zero mean random small perturbation,[24] the Duffing oscillator detection system based on the small-scale periodic state is proposed. Then, using the phase trajectory characteristics, a new method for weak wide-band signal frequency detection based on this system is also proposed. This method not only overcomes the disadvantages of a conventional Duffing oscillator detection method which is based on a strong reference signal, but also realizes the frequency detection of wide-band signals using a simpler structure. Finally, we investigated the performance of the proposed method. Simulation results show that this approach can achieve a lower SNR detection threshold, which provides a new solution for Duffing oscillator weak wide-band signal detection.

The rest of this paper is organized as follows. Section 2 gives a preliminary description of the Duffing oscillator system in a small-scale periodic state. In Section 3, a weak signal frequency detection method based on the small-scale periodic state of Duffing oscillator is presented together with MATLAB simulations. In Section 4, the performance of the proposed method is evaluated by simulations. Finally, conclusions are presented in Section 5.

2. Weak signal detection system based on the Duffing oscillator

2.1. Theory of the stopping oscillation system

The stochastic differential equation can be given as[24]

$$\begin{cases} D^q \boldsymbol{X} = \boldsymbol{F}(X,t) + e\xi(t), \\ \boldsymbol{X}(t_0) = \boldsymbol{x}_0, \end{cases} \tag{1}$$

where $\boldsymbol{X}$ and $\boldsymbol{F}$ are both two-dimensional vector stochastic processes; $q \in \boldsymbol{R}$ is the order of the differential equation, $e\xi(t)$ is a random perturbation from system inputs, where e is the amplitude; and η_0 is the trivial solution (i.e., $\boldsymbol{F}(\eta_0, t) = 0$).

s.t.

i) $\lim\limits_{\|x_0-\eta_0\|\to 0} P\left\{\lim\limits_{\substack{t\to\infty \\ e\to 0}} \|\boldsymbol{X}(t;t_0,\boldsymbol{x}_0)-\eta_0\|\right\} = 1.$

ii) When the input is a periodic signal, equation (1) has a periodic or quasi-periodic solution.

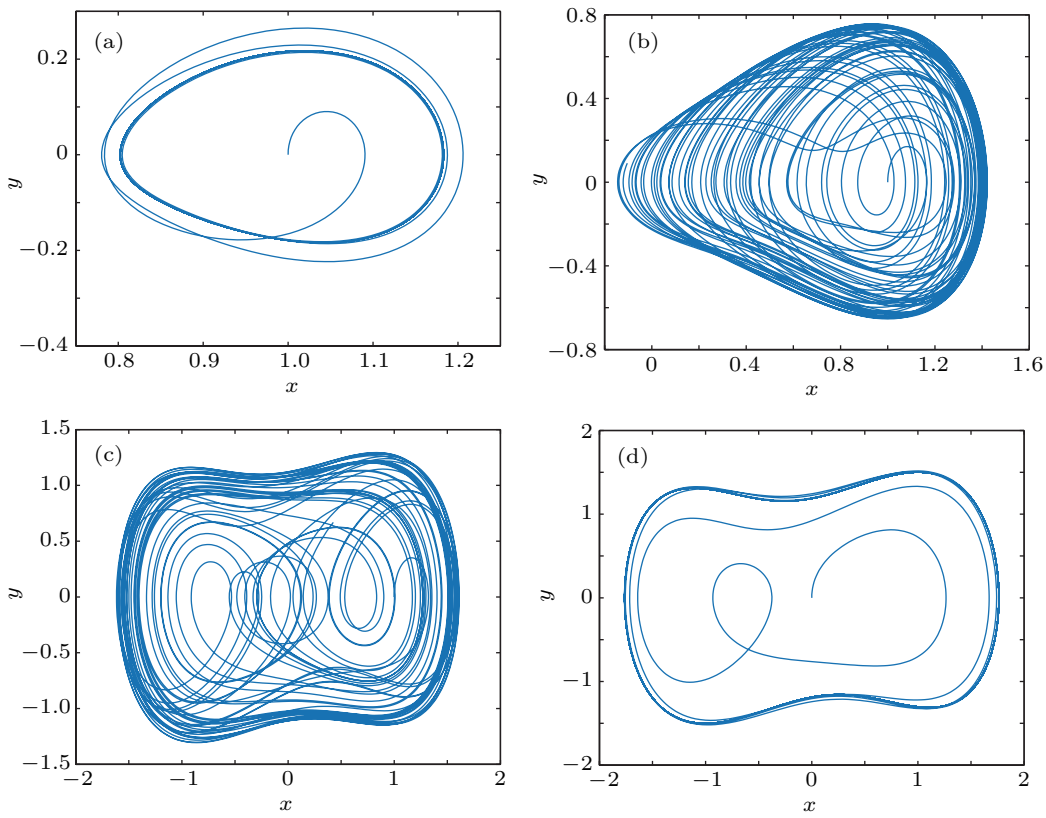


Fig. 1. (color online) Phase trajectories of the Duffing oscillator system at $k = 0.5$. (a) $\gamma = 0.3$, small-scale periodic motion; (b) $\gamma = 0.5$, double-periodic motion; (c) $\gamma = 0.82$, chaotic motion; (d) $\gamma = 0.83$, large-scale periodic motion.

Under this circumstance, the system corresponding to Eq. (1) is called the stopping oscillation system.[24] Condition i) indicates that the system is asymptotically stable with probability 1 when the input is a small random perturbation, and the corresponding state is called the stopping oscillation state. Condition ii) indicates that the system is in a periodic or quasi-periodic state when the input is a periodic signal.

According to the definition, in the stopping oscillation system, the state transition from stopping oscillation state to periodic or quasi-periodic state is sensitive to a periodic signal and immune to noise. Thus, it provides a new idea for detecting weak periodic signals with unknown frequencies.

2.2. Principles of the Duffing oscillator

The conventional Duffing oscillator detection system based on a strong reference signal can be described by the following equation:[25,26]

$$\ddot{x}(t)+k\dot{x}(t)-x(t)+x^3(t)=\gamma\cos(\omega t), \tag{2}$$

where k is the damping ratio, $-x(t)+x^3(t)$ is the non-linear recovery force, and $\gamma\cos(\omega t)$ is the reference signal. For fixed $k=0.5$, with an increase of γ, the Duffing oscillator varies from small-scale periodic motion to double-periodic motion and then to chaotic motion. When γ increases to a value slightly greater than the critical threshold γ_c, the system transforms to large-scale periodic motion through the critical state (chaos, but on the verge of changing to the large-scale periodic motion), as shown in Fig. 1.

Using the conventional Duffing oscillator detection method which is based on a strong reference signal, a weak periodic signal buried in noise can be detected via the phase transition from chaos to large-scale periodic motion.[27]

However, there are several inherent deficiencies in the conventional Duffing oscillator detection method.

i) There is a non-detection zone when detecting a weak signal with a frequency which is identical to the reference signal frequency. In this zone, the system always remains in chaotic motion, which means that the signal cannot be detected by the phase transition.[22]

ii) The critical threshold varies with the reference signal frequency and the intensity of the background noise.[23]

iii) The frequency detection interval of a single Duffing oscillator is very narrow. Therefore, for an unknown weak signal, an array of uncoupled Duffing oscillators must be used to cover the whole frequency domain, but it may also lead to greater computational cost and time in the process.

iv) There is a transition section in the transition process from the initial value or chaotic motion to the large-scale periodic motion. Therefore, more time is required to determine the current state of the system. Otherwise, this may lead to misjudgment, and to a reduction of the detection accuracy.[28]

2.3. Characteristics of the Duffing oscillator in small-scale periodic state

To eschew these deficiencies without the reference signal, a weak signal detection system driven only by a to-be-detected signal buried in noise, can be given as

$$\ddot{x}(t)+k\dot{x}(t)-x(t)+x^3(t)=A\cos(\omega_0 t+\varphi)+n(t), \tag{3}$$

where $A\cos(\omega_0 t+\varphi)$ is the to-be-detected signal (the driving force), and $n(t)$ is the Gaussian white noise.

Generally, an equivalent transformation of Eq. (3) is performed to detect a signal with an arbitrary frequency, its state equation can be given as

$$\begin{cases}\dot{x}=\omega y,\\ \dot{y}=\omega(-ky+x-x^3+A\cos(\omega_0 t+\varphi)+n(t)),\end{cases} \tag{4}$$

where ω is the angular frequency of the reference signal. To ensure that the Duffing oscillator system works in the small-scale periodic state, the value of A cannot exceed 0.36.[29,30]

Based on Hamiltonian system theory, when $k>0$, driven only by Gaussian white noise, the Duffing oscillator system in Eq. (4) satisfies condition 1) of Eq. (1); while it is a dissipation system when driven by a periodic signal.[31,32] Therefore, when $k>0$, the Duffing oscillator system in Eq. (4) is a stopping oscillation system and can be used for weak signal detection.

The phase trajectories of the Duffing oscillator system in Eq. (4) are shown in Fig. 2. Driven by the Gaussian white noise $n(t)\sim N(0,0.1^2)$ with zero mean value and the variance of 0.1^2, the system is asymptotically stable with probability 1, that is, the system is in the stopping oscillation state (see Fig. 2(a)). Driven by the sinusoidal signal, the system has a periodic solution, i.e., this system immediately changes from the stopping oscillation state to the small-scale periodic state (see Fig. 2(b)). Figure 2 also shows that regardless of the system's state, the focus of the phase trajectory is (1, 0).

To facilitate the subsequent analysis and calculations, it is necessary to make the phase points uniformly distributed in four quadrants as far as possible. Thus, equation (4) can be modified as Eq. (5) to make the phase trajectory focus on (0, 0).

$$\begin{cases}\dot{x}=\omega y,\\ \dot{y}=\omega(-ky+(x+1)-(x+1)^3\\ \qquad +A\cos(\omega_0 t+\varphi)+n(t)).\end{cases} \tag{5}$$

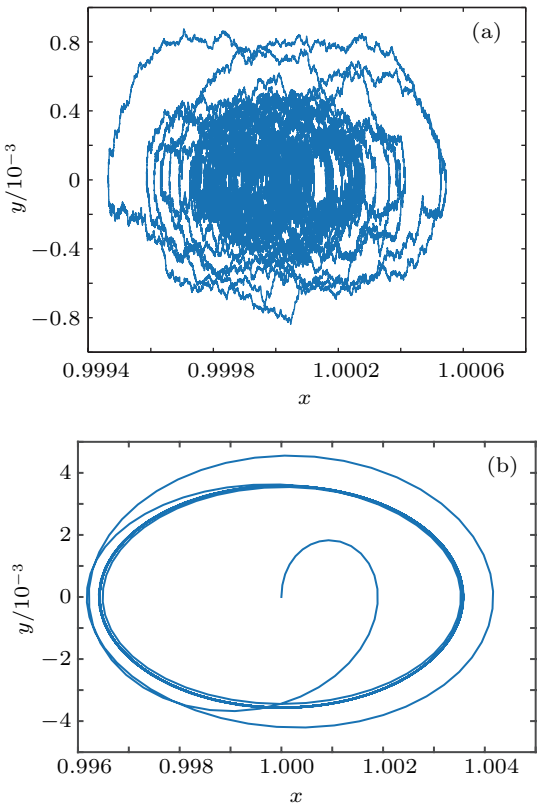


Fig. 2. (color online) Phase trajectories of the system in Eq. (4) driven by (a) Gaussian white noise $n(t) \sim N(0, 0.1^2)$; (b) sinusoidal signal $0.004\cos(2\pi \times 1000t)$.

In this paper, the Duffing oscillator system in a small-scale periodic state in Eq. (5) is used for weak signal detection. Herein, we use the standard definition of the SNR in the logarithm form as follows:

$$\mathrm{SNR} = 10\log\left(\frac{A^2}{2\sigma^2}\right), \tag{6}$$

where A is the amplitude of the to-be-detected signal, and σ^2 is the noise variance. Figure 3 shows the phase trajectories of the Duffing oscillator system in Eq. (5) when driven by different signals. When driven by Gaussian white noise, figure 3(a) indicates that the system is in the stopping oscillation state. Figure 3(b) shows the system is in the small-scale periodic state when it is driven only by a weak periodic signal $0.004\cos(2\pi \times 1000t)$. The addition of strong noise to this system when the SNR is -45 dB does not result in a change in the system's state as shown in Fig. 3(c), although the local phase trajectory becomes rough. Therefore, even if the SNR is very low, the system in Eq. (5) is still sensitive to a specific signal and immune to random perturbations by simulation. The phase transition from the stopping oscillation state to the small-scale periodic state in the Duffing oscillator system can then be used to detect the existence of a weak periodic signal.

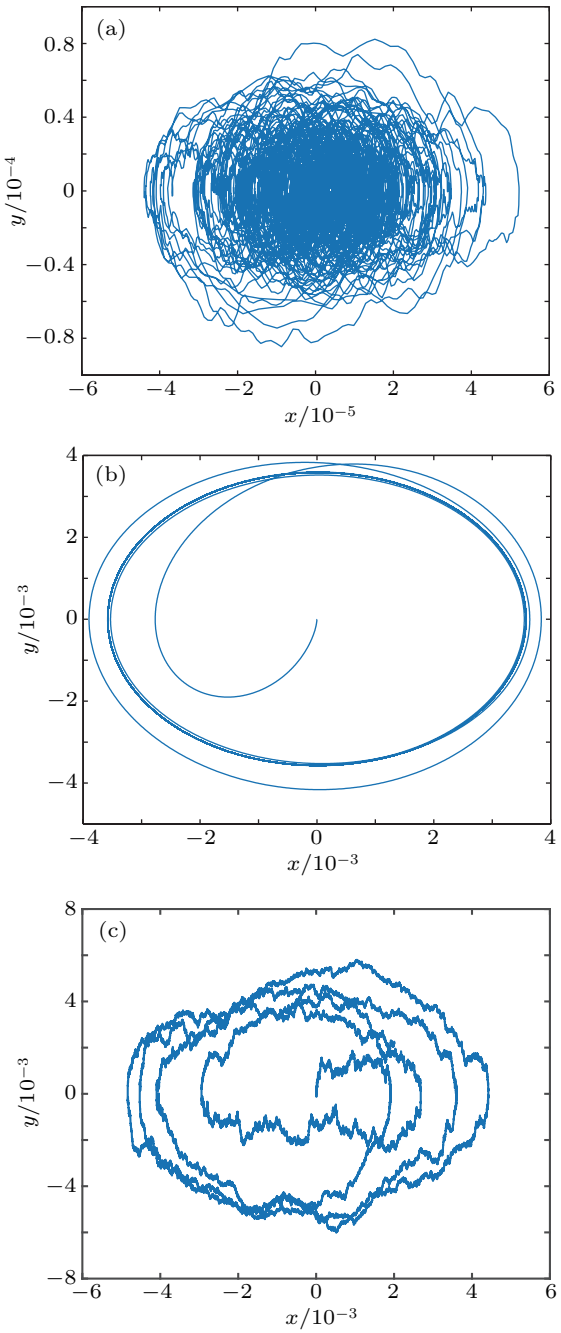


Fig. 3. (color online) Phase trajectories of the system in Eq. (5) driven by (a) Gaussian white noise $n(t) \sim N(0, 0.1^2)$; (b) sinusoidal signal $0.004\cos(2\pi \times 1000t)$ without noise; (c) sinusoidal signal at -45 dB of SNR.

3. Weak signal detection method based on the small-scale periodic state

In Section 2, the characteristics of the Duffing oscillator in a small-scale periodic state are investigated, and it is demonstrated that this system is suitable for weak signal detection both from theoretical analysis and simulation results.

A large number of simulation results reveal that the phase trajectory is irregular when the system is in the stopping oscillation state; while the phase trajectory is regular when the system is in the small-scale periodic state. More importantly, when the Duffing oscillator system is in the latter state,

the phase trajectory has the same periodicity with the to-be-detected signal. Using this knowledge, the phase space angle can be used for weak periodic signal detection.

Defining ϕ as the phase space angle corresponding to the phase point (x,y) in the phase plane, the sine and cosine functions of ϕ can be given as

$$\sin\phi = \frac{x}{\sqrt{x^2+y^2}}, \quad \cos\phi = \frac{y}{\sqrt{x^2+y^2}}. \tag{7}$$

It is well known that x and y are the displacement and velocity of the Duffing oscillator, respectively. Therefore, the periodic characteristics of the phase trajectory can be described using sine and cosine functions.

Setting the system initial value $(x,y) = (0,0)$, and adding the to-be-detected signal $0.004\cos(2\pi \times 1000t)$ with different SNRs into the detection system in Eq. (5), figure 4 shows the corresponding relationship among the time series of the to-be-detected signal and the sine cosine curves of the phase space angles. Without noise, or when the SNR is not less than -20 dB, the to-be-detected signal and the sine cosine curves have the same period (see Figs. 4(a) and 4(b)). When the noise intensity is increased so the point that the SNR reaches -45 dB, the time series of the to-be-detected signal is not clearly identified, but the sine cosine curves are still relatively clear (see Fig. 4(c)). A further increase of the noise intensity level results in the complication of all three curves, and their corresponding relationship is difficult to obtain at -50 dB of SNR (see Fig. 4(d)).

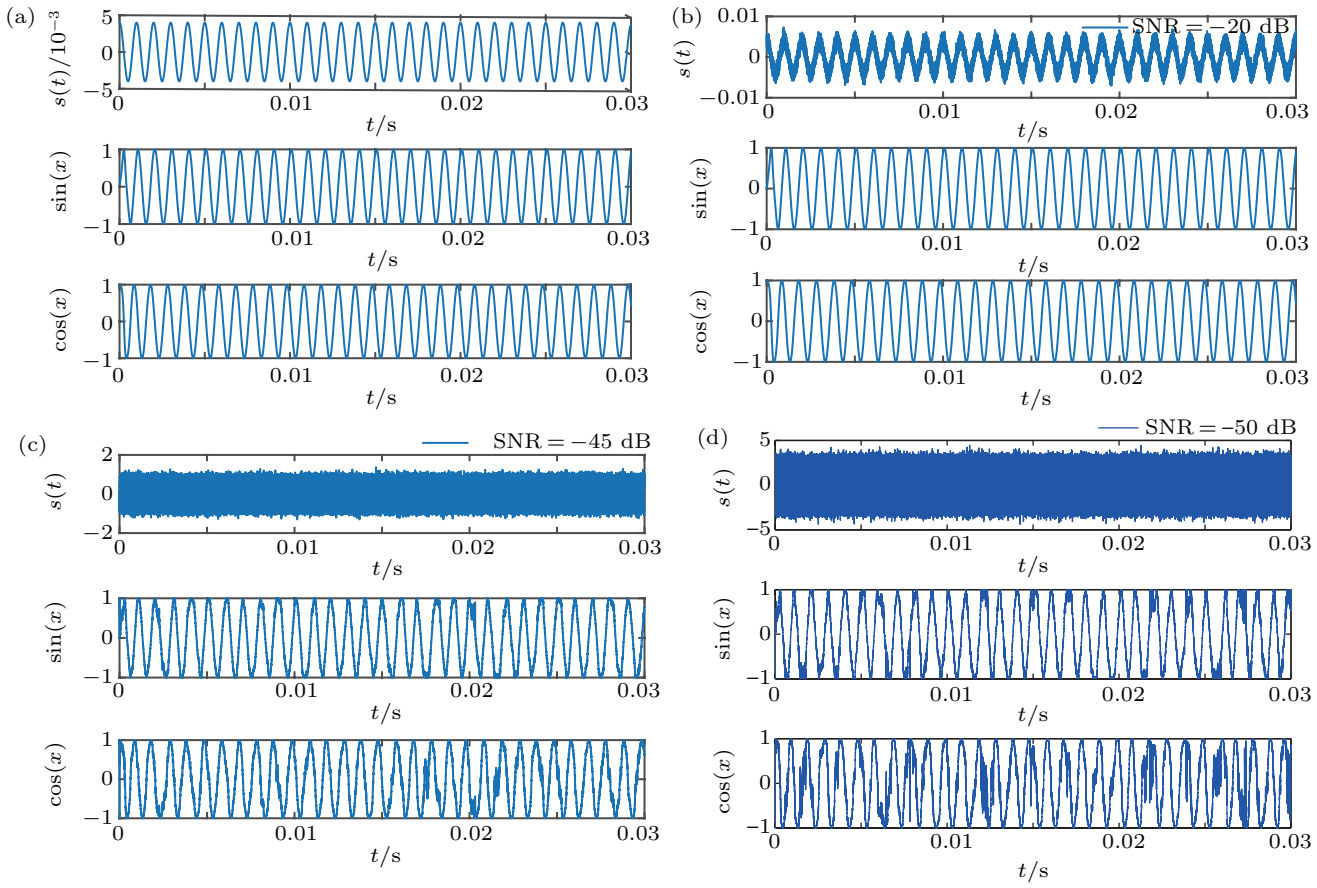


Fig. 4. (color online) Time series of the to-be-detected signal and the sine cosine curves (a) sinusoidal signal $0.004\cos(2\pi \times 1000t)$ without noise; (b) at -20 dB of SNR; (c) at -45 dB of SNR; (d) at -50 dB of SNR.

From the above analysis, it can be found that even though the noise intensity is large, the sine cosine curves can still accurately reflect the frequencies of the to-be-detected signals. Therefore, when the Duffing oscillator is in the small-scale periodic state and the SNR is higher than -50 dB, we can use sine cosine curves for frequency detection.

In addition, when the frequency difference between the reference signal and the to-be-detected signal is too large, the output (x,y) of the Duffing oscillator cannot respond well to the rapid changes of the to-be-detected signal, and the periodic characteristics of the small-scale periodic state would be destroyed. As seen in Fig. 5, a larger frequency difference between the two signals causes both the displacement and the velocity to deviate from the origin (0, 0), where the deviation of the displacement is even larger than that due of the velocity. This means that the influence of noise on the displacement is greater than the influence on the velocity. To conclude, in order to decrease the influence of a large frequency difference, the cosine function of the phase space angles is used to detect the to-be-detected signal frequency in this report. More im-

portantly, for the detection of weak signals with different frequencies, we must estimate the approximate frequency range $[\omega_{0\text{start}}, \omega_{0\text{end}}]$ of the to-be-detected signal first, and then select an appropriate reference signal frequency according to this pre-estimated frequency range to ensure that the frequency difference is not too large.

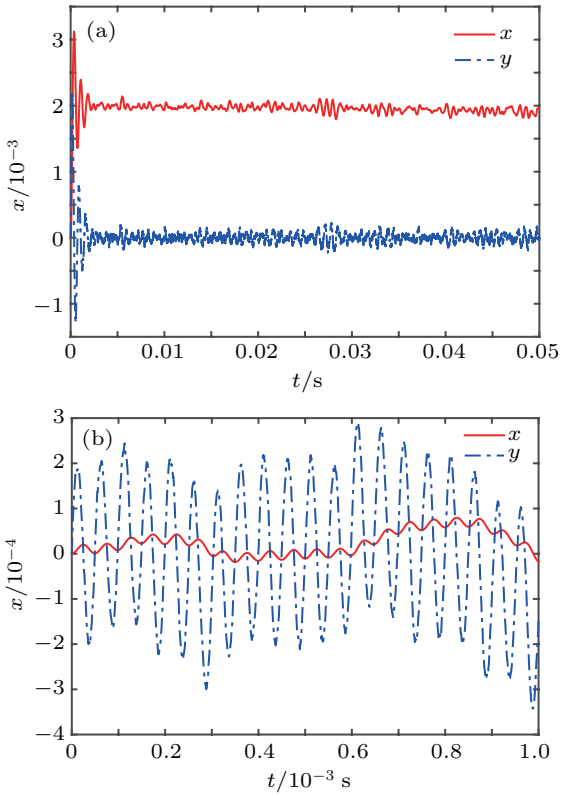


Fig. 5. Time series of (x, y) when (a) $\omega_0 \ll \omega$; (b) $\omega_0 \gg \omega$.

Based on the above studies, a novel Duffing oscillator weak signal detection method based on the small-scale periodic state is proposed to detect weak wide-band signals. The specific implementation can be described as follows.

i) Initializing the parameters: initial value of the Duffing system (0, 0), the damping ratio $k = 0.5$.

ii) Selecting a value within $[\omega_{0\text{start}}, \omega_{0\text{end}}]$ as the reference signal angular frequency to obtain a small frequency difference between the reference signal and the to-be-detected signal.

iii) Adding the to-be-detected signal buried in noise to the Duffing oscillator system in the small-scale periodic state in Eq. (5), and calculating the corresponding cosine value using Eq. (7).

iv) Setting the starting point of the search data to avoid the influence of the transition section on the frequency detection accuracy. Then, using the peaks of the cosine curve and its corresponding time series to calculate the cosine curve frequency, which is considered to be the measured value of the to-be-detected signal frequency.

Furthermore, we can detect periodic signals in different frequency bands by changing the reference signal frequency.

4. Numerical experiments and analysis

In this section, three scenarios are considered which include the Duffing oscillator system is driven by (i) periodic signals, (ii) divergent or attenuation oscillator signals, and (iii) chirp signals. For each scenario, the initial value of the Duffing oscillator systems is $(x, y) = (0, 0)$, the reference signal angular frequency is $\omega = 2\pi f = 2\pi \times 1000$ rad/s, and the frequency detection accuracy can be given as

$$\eta = 1 - \frac{|\omega_0 - \omega_0'|}{\omega_0}, \tag{8}$$

where ω_0 and ω_0' are the real value and measured value of the to-be-detected signal angular frequencies, respectively.

4.1. Weak periodic signals detection

In the first scenario, the periodic signal is used as a driving force and added to the Duffing oscillator system in Eq. (5), which can be given as

$$s_1(t) = A\cos(\omega_0 t) = 0.004\cos(2\pi f_0 t), \tag{9}$$

where $s_1(t)$ is the to-be-detected periodic signal.

Table 1. Frequency detection intervals of a single Duffing oscillator driven by periodic signals at different SNRs. The notation – implies that the detection failed.

f/Hz	SNR/dB	Small-scale periodic		Strong reference signal	
		f_L/Hz	f_H/Hz	f_L/Hz	f_H/Hz
1000	0	1	166000	973.8	1033.3
1000	–10	1	85000	973.8	1033.3
1000	–20	50	6000	973.8	1033.3
1000	–30	140	4000	973.8	1033.3
1000	–40	430	2100	–	–
1000	–45	900	1800	–	–

For to-be-detected periodic signals, Table 1 shows the frequency detection intervals $[f_L, f_H]$ of a single Duffing oscillator using the Duffing oscillator detection method based on the small-scale periodic state and a strong reference signal. All of the frequency detection accuracies in these intervals are higher than 99%. Considering the detection method based on the small-scale periodic state, the frequency detection interval of a single Duffing oscillator is very wide. However, based on a strong reference signal, the frequency detection interval of a single Duffing oscillator is limited, that is, the regular intermittent chaos will take place and can be used for frequency detection only when the relative frequency difference is less than 0.03.[15] An increase in the noise intensity leads to a small

amount of transient chaotic motions entering the phase trajectory. Thus, the regular intermittent chaos no longer occurs, and the strong reference signal method cannot be used for frequency detection at −30 dB of the SNR. However, based on the small-scale periodic state method, although the decrease of the SNR results in narrower frequency detection intervals, the intervals are still much larger than those of the detection method based on a strong reference signal in Ref. [15]. As already demonstrated in this report, the proposed method greatly expands the frequency detection interval of a single Duffing oscillator. Thus, instead of an array of uncoupled Duffing oscillators, we can detect the existence of a weak wide-band signal and obtain its frequency using a single Duffing oscillator with a faster speed, using the phase transition from the stopping oscillation state to the small-scale periodic state. In addition, there is no strict limit to the reference signal frequency in the proposed method, as long as it is within the pre-estimated frequency range $[\omega_{0\text{start}}, \omega_{0\text{end}}]$ of the to-be-detected signal.

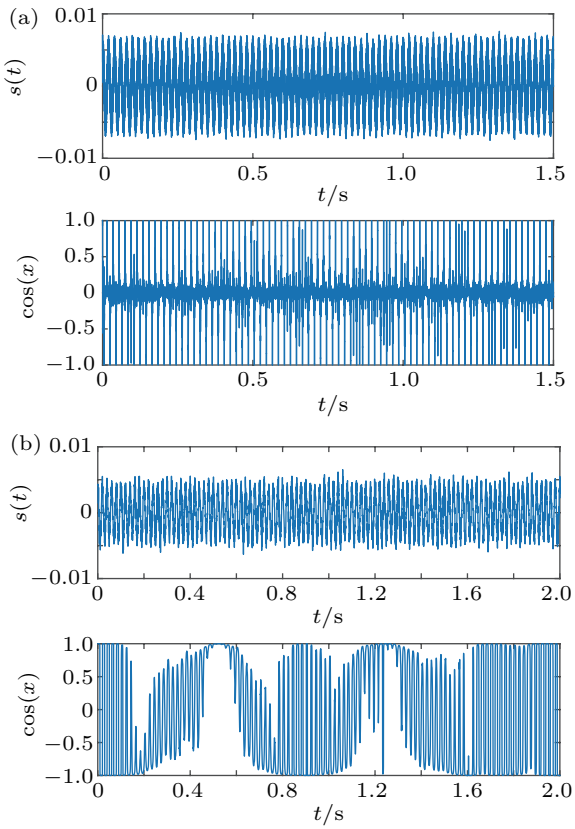


Fig. 6. Time series of the to-be-detected signal and cosine function when (a) $f_0 < f_L$; (b) $f_0 > f_H$.

When the to-be-detected signal frequency is outside the frequency detection interval, figure 6 shows that the characteristic of having the same period between the cosine curves and the to-be-detected signal will be abruptly deteriorated. Furthermore, as seen in Fig. 7, the phase trajectories become irregular spiral curves and cannot maintain the small-scale periodic state. This is because the system's output (x, y) decreases rapidly when the frequency difference is too large, so that the influence of noise is more prominent. This greatly reduces the frequency detection accuracy. Therefore, it is no longer suitable for frequency detection when the frequency difference is too large.

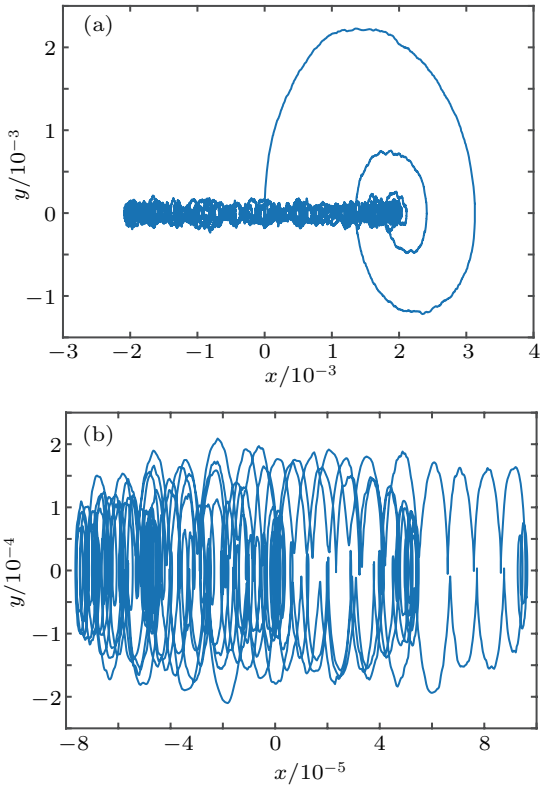


Fig. 7. Phase trajectories when (a) $f_0 < f_L$; (b) $f_0 > f_H$.

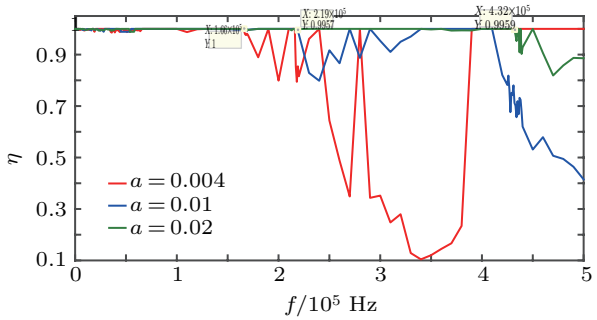


Fig. 8. Frequency detection accuracies (η) of periodic signals with different amplitudes.

The influence of the to-be-detected signal amplitudes on the frequency detection intervals of a single Duffing oscillator also needs to be discussed. For example, when the SNR is 0 dB, keeping other parameters unchanged and increasing A to 0.01 or 0.02 from 0.004, respectively, as seen in Fig. 8, f_L remains at 1 Hz, and f_H increases to 219 kHz and 432 kHz from 166 kHz correspondingly. In summary, frequency detection intervals $[f_L, f_H]$ extends with an increase of the amplitude. This is mainly because a larger amplitude requires the system to have a longer time to maintain the stability of the small-scale periodic state.

4.2. Weak divergent and attenuation signals detection

In the second scenario, the divergent or attenuation oscillation signals are used as driving forces, and are given as

$$s_2(t) = Ae^{0.1t}\cos(\omega_0 t) = 0.004e^{0.1t}\cos(2\pi f_0 t), \quad (10)$$

$$s_3(t) = Ae^{-0.1t}\cos(\omega_0 t) = 0.004e^{-0.1t}\cos(2\pi f_0 t), \quad (11)$$

where $s_2(t)$ is the to-be-detected divergent oscillation signal, and $s_3(t)$ is the to-be-detected attenuation oscillation signal.

Adding the divergent oscillation signal as a driving force to the Duffing oscillator system in Eq. (5), it can be seen from Fig. 9(a) that the system maintains the small-scale periodic state, and the phase trajectory spirally diverges from the initial value. When the amplitude of the input signal exceeds the threshold of 0.36, the phase transition from the small-scale periodic state with slowing increasing amplitude to the double-periodic state takes place, as shown in Fig. 9(b). Therefore, the to-be-detected signal should be multiplied by a weighting factor ε $(0 < \varepsilon < 1)$ to ensure that the system is in the small-scale periodic state.

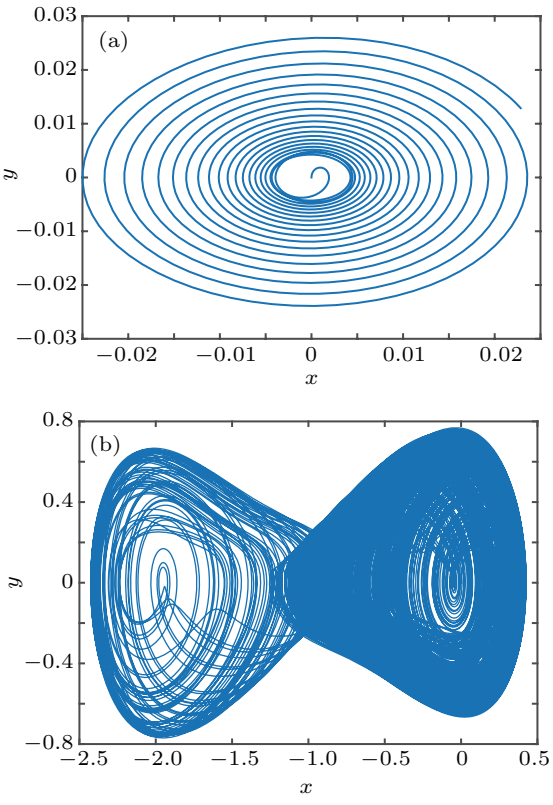


Fig. 9. Phase trajectories driven by the divergent oscillation signals in (a) small-scale periodic motion; (b) double-periodic motion.

Similarly, taking the attenuation oscillation signal as a driving force, figure 10 shows the system maintains the small-scale periodic state, and the phase trajectory spirally shrinks from the initial value. If the simulation time is sufficiently long, the amplitude of the input signal will be reduced to an infinitely small value, and the Duffing oscillator system will be infinitely close to the stopping oscillation state. However, the weak signal frequency detection method proposed in this paper only requires a few cycles, and the signal amplitude changes slowly during this time. Therefore, the proposed method can meet the requirements for detection accuracy and real-time performance.

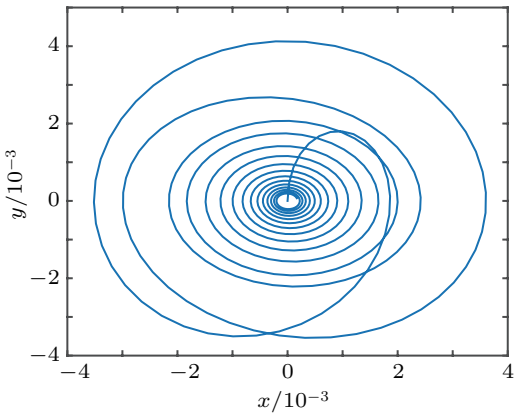


Fig. 10. Phase trajectory driven by an attenuation oscillation signal.

Figure 11 shows the frequency detection accuracies for the periodic signal, the divergent and the attenuation oscillation signal, with $A = 0.004$ and -45 dB of SNR. It can be seen that in all cases, the frequency detection accuracy can exceed 99% in the frequency interval [900 Hz, 1800 Hz] when driven by the periodic signal. When driven by the divergent oscillation signal, the frequency detection interval is expanded to [850 Hz, 1950 Hz]. The frequency detection interval is reduced to [950 Hz, 1620 Hz], when the attenuation oscillation signal is used as a driving force.

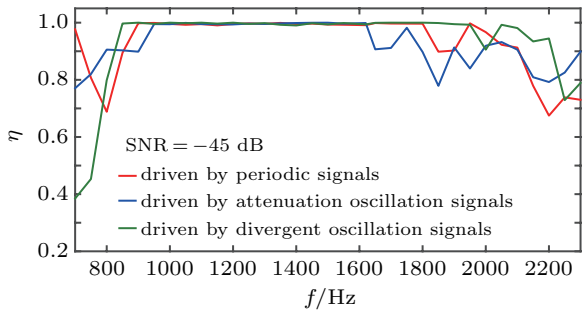


Fig. 11. Frequency detection accuracy (η) for different driving signals.

For divergent or attenuation oscillation signals, in order to compare the detection ability of the proposed method with the detection method based on a strong reference signal, Tables 2 and 3 provide the frequency detection intervals of a single Duffing oscillator at different SNRs. When the SNR is higher than -20 dB, both methods can be used for frequency detection, but the proposed method presents wider frequency detection intervals. When the SNR is less than -20 dB, the method proposed in this paper has a better detection rate. However, the detection method based on a strong reference signal fails

to do it because the regular intermittent chaotic phenomenon no longer occurs. In addition, compared to the frequency detection intervals driven by the periodic signals in Table 1, it can be concluded that, when the divergent oscillation signal is used as a driving force, the slow increase of the amplitude leads to an increase of the frequency detection interval. However, when using the attenuation oscillation signal as the driving force, the frequency detection interval drops slightly although the drop scope is very small, due to the slow decrease of the amplitude. Therefore, compared with the conventional method, the proposed method can accurately obtain the frequencies of divergent and attenuation oscillation signals in a wider frequency band and a lower SNR.

Table 2. Frequency detection intervals of a single Duffing oscillator driven by divergent oscillation signals. The notation – implies the detection failed.

f/Hz	SNR/dB	Small-scale periodic state		Strong reference signal method	
		f_L/Hz	f_H/Hz	f_L/Hz	f_H/Hz
1000	0	1	167000	973.8	1033.3
1000	–10	20	86000	973.8	1033.3
1000	–20	40	6300	–	–
1000	–40	420	2300	–	–
1000	–45	850	1950	–	–

Table 3. Frequency detection intervals of a single Duffing oscillator driven by attenuation oscillation signals. The notation – implies the detection failed.

f/Hz	SNR/dB	Small-scale periodic state		Strong reference signal method	
		f_L/Hz	f_H/Hz	f_L/Hz	f_H/Hz
1000	0	1	165000	973.8	1033.3
1000	–10	20	84000	973.8	1033.3
1000	–20	50	5700	–	–
1000	–40	450	2000	–	–
1000	–45	950	1620	–	–

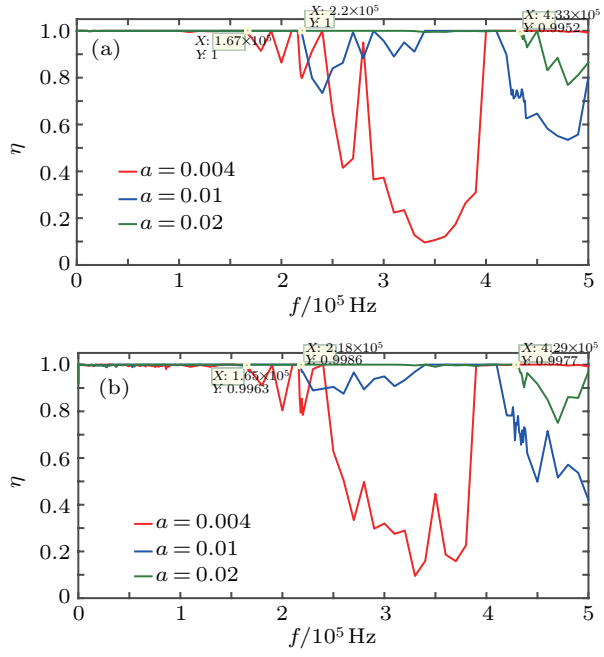


Fig. 12. Effect of initial amplitudes on frequency detection accuracy (η) when the driving signals are (a) divergent oscillation signals and (b) attenuation oscillation signals.

In addition, to study the influence of the initial amplitude on the frequency detection intervals of a single Duffing oscillator, figure 12 shows a series of frequency detection accuracy curves for divergent and attenuation oscillation signals with initial amplitudes A of 0.004, 0.01, and 0.02. According to Fig. 12, the curves with different amplitudes have similar behavior, that is, the frequency detection intervals extend with an increase of the initial amplitude. In addition, compared with the frequency detection intervals for periodic signals as shown in Fig. 8, when the driving forces are divergent oscillating signals, the frequency detection intervals with different initial amplitudes are increased. In the case of the attenuation oscillation signals, all the frequency detection intervals are reduced.

4.3. Weak chirp signals detection

In the last scenario, the chirp signal is used as a driving force, which can be given as

$$\begin{aligned} s_4(t) &= A\cos 2\pi(f_0 + 0.5bt)t \\ &= 0.004\cos 2\pi(1000t + 0.5bt^2), \end{aligned} \tag{12}$$

where the initial frequency of the to-be-detected chirp signal $s_4(t)$ is 1000 Hz, and b is the frequency change rate. For example, when $b = 2000$, figure 13 shows that the phase trajectory occupies much more space in the phase space compared with the phase trajectory driven by a periodic signal. However, the phase trajectory is still in the small-scale periodic state and can

be used for frequency detection by the proposed method.

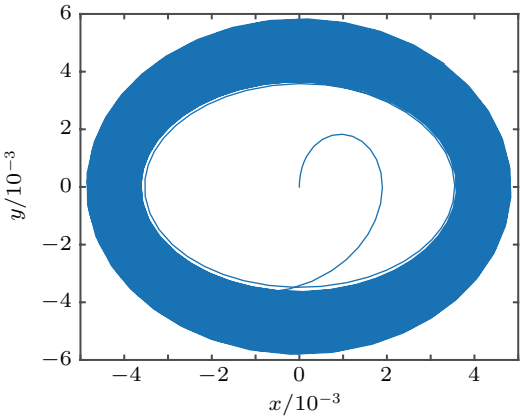


Fig. 13. Phase trajectory driven by a chirp signal.

Adding chirp signals with different frequency change rates to the Duffing oscillator system in Eq. (5), figure 14 reveals that when the SNR is not less than −20 dB, and the frequency change rate is between 1 Hz/s to 2500 Hz/s, the detection accuracy of the initial frequencies is higher than 99%. The frequency detection accuracy decreases with an increase of the noise intensity and frequency change rate. When the SNR is between −25 dB and −45 dB, the maximum value of b is 2000 Hz/s in order to ensure the stability of detection accuracy. If b is too large, then the instantaneous frequencies of the to-be-detected signals may exceed the frequency detection intervals, which lead to a decrease of the system's detection accuracy and stability.

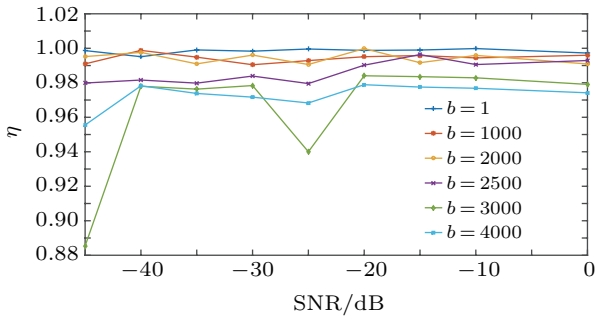


Fig. 14. Frequency detection accuracy (η) for chirp signals based on the small-scale periodic state of the Duffing oscillator.

Using the conventional detection method based on a strong reference signal, we can obtain the frequency of the to-be-detected signal only when the SNR is not less than −20 dB and the frequency change rate is less than 15. Otherwise, this approach cannot complete the chirp signal frequency detection, as shown in Fig. 15. This is due to the fact that when the reference signal frequency is fixed, the resulting rapid frequency change will result in a large frequency difference, so the regular intermittent chaotic motion cannot take place. Therefore, for chirp signals, a better frequency detection rate can be achieved using the proposed method.

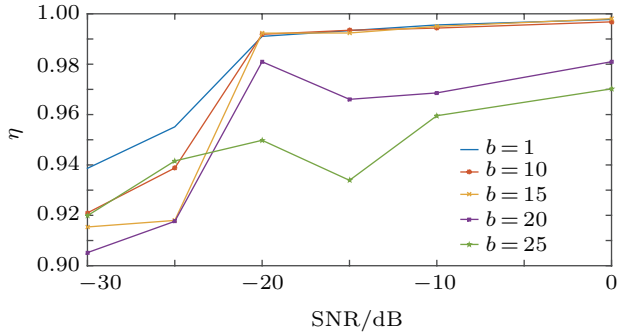


Fig. 15. Frequency detection accuracies for (η) chirp signals based on a strong reference signal.

Besides, instead of an array of uncoupled Duffing oscillators, the proposed method only requires a single Duffing oscillator for weak signal detection which has a significantly lower computational burden compared to the method based on a strong reference signal.

5. Conclusion

In this paper, a weak wide-band signal detection method based on the small-scale periodic state of a Duffing oscillator is proposed. In order to eschew the deficiencies of a conventional Duffing oscillator detection method based on a strong reference signal, the to-be-detected signal buried in noise is considered as the driving force. Then, the cosine function of the phase space angles was used to detect the weak signal frequency when the system is in the small-scale periodic state. Simulation results demonstrate that the frequency detection interval of a single Duffing oscillator was significantly improved, which means that the proposed method is more suitable for detecting the existence of a weak wide-band signal and extracting its frequency with a higher speed. In addition, the approach reduces the detection threshold of the input SNR and improves the detection accuracy and real-time performance.

It is noteworthy that the frequency detection interval of a single Duffing oscillator is reduced when the SNR is low, which improves the adaptability of the reference signal frequency. By modifying the developed algorithm, the frequency detection interval could be further expanded.

References

[1] Zhang J and Zhang T 2015 *Rev. Sci. Instrum.* **86** 025005
[2] Hänggi P 2002 *Chemphyschem* **3** 285
[3] Li Y and Yang B J 2004 *Chaotic Oscillator Detection Introduction* (Beijing: Publishing House of Electronics Industry) p. 29 (in Chinese)
[4] Xu Y C, Yang C L and Qu X D 2010 *Chin. Phys. B* **19** 030516

[5] Lai Z H and Leng Y G 2016 *Mech. Syst. Signal. Pr.* **81** 60
[6] Zhao Z K, Wang X and Zhang X G 2014 *Adv. Mech. Eng.* **2014** 1
[7] Wu J, Wang Y, Zhang W, Nie Z, Lin R and Ma H 2016 *Mech. Syst. Signal. Pr.* **82** 130
[8] Birx D L and Pipenberg S J 1992 *International Joint Conference on Neural Networks*, June 7–11, 1992, Baltimore, MD, USA, p. 881
[9] Permann D and Hamilton I I 1992 *Phys. Rev. Lett.* **69** 2607
[10] Zhao Z Z and Yang S P 2015 *Comput. Electr. Eng.* **41** 1
[11] Peng H H, Xu X M, Yang B C and Yin L Z 2016 *J. Phys. Soc. Jpn.* **85** 044005
[12] Hu N Q and Wen X S 2003 *J. Sound Vib.* **268** 917
[13] Shi H, Fan S, Xing W and Sun J 2015 *Mech. Syst. Signal Process.* **50** 535
[14] Costa A H, Enríquez-Caldera R, Tello-Bello M and Bermúdez-Gómez C R 2016 *Digit. Signal Process.* **55** 32
[15] Wang G Y, Chen D J, Lin J Y and Chen X 1999 *IEEE Trans. Ind. Electron.* **46** 440
[16] Wang G Y and He S 2003 *IEEE Trans. Circ. Syst.* **50** 945
[17] Li Y, Lu P, Yang B J and Zhao X P 2006 *Acta Phys. Sin.* **55** 1672 (in Chinese)
[18] Nie C Y and Shi Y W 2001 *Chin. J. Sci. Instrum.* **22** 33
[19] Zeng Z Z, Zhou Y and Hu K 2015 *Acta Phys. Sin.* **64** 070505 (in Chinese)
[20] Lai Z H and Leng Y G 2015 *Sensors* **15** 21327
[21] Rashtchi V and Nourazar M 2015 *Circuits Syst. Signal Process.* **34** 3101
[22] Li Y, Yang B J, Lin H B and Liu X X 2005 *Acta Phys. Sin.* **54** 1994 (in Chinese)
[23] Fan J, Zhao W L and Wang W Q 2013 *Acta Phys. Sin.* **62** 080502 (in Chinese)
[24] Zhou X X, Lai L and Luo M K 2013 *Acta Phys. Sin.* **62** 090501 (in Chinese)
[25] Shaw S W and Holmes P J 1983 *J. Sound. Vib.* **90** 129
[26] Wiggins S 1987 *Phys. Lett. A* **124** 138
[27] Yan B N, Liu C X, Ni J K and Zhao L 2016 *Chin. Phys. B* **25** 100502
[28] Liu H B, Wu D W, Jin W and Wang Y Q 2013 *Acta Phys. Sin.* **62** 050501 (in Chinese)
[29] Li M P, Xu X M, Yang B C and Ding J F 2015 *Chin. Phys. B* **24** 060504
[30] Lai Z H, Leng Y G, Sun J Q and Fan S B 2012 *Acta Phys. Sin.* **61** 60 (in Chinese)
[31] Zhu W Q 2003 *Nonlinear Stochastic Dynamical Systems and Control* (Beijing: Science Press) pp. 330–335
[32] Zhang Z F, Ding T R, Huang W Z and Dong Z X 1997 *Qualitative Theory of Differential Equation,* 2nd end (Beijing: Science Press) pp. 450–451